

# Fundamental Brain Research

Thomas F. Quatieri, Laura J. Brattain, Todd A. Thorsen, Gregory A. Ciccarelli, Shaun R. Berry, Jeffrey S. Palmer, Satrajit S. Ghosh, and Kwanghun Chung

The brain is a marvel of biological engineering that, if understood well, could yield unprecedented breakthroughs in treatments for neuropsychological diseases. To further develop scientists' knowledge of the brain, Lincoln Laboratory and MIT campus have teamed up in several areas of fundamental brain research. Together, we are pushing the boundaries of novel imaging and neural manipulation techniques and codifying our knowledge with neurocomputational models.



**The human brain is an astoundingly** complex structure that contains tens of billions of neurons connected through trillions of synapses. This circuitry is the result of our genome, development, learning, and experience, and it governs the brain's functioning. At Lincoln Laboratory, in collaboration with MIT campus, we are developing novel approaches to measuring, manipulating, and modeling the brain's structure and function. Our ultimate goal is to improve scientists' understanding of the brain and to discover advanced methods to detect, monitor, and treat neurological and neurodevelopmental conditions, such as depression, dementia, Parkinson's disease, and autism spectrum disorders. Our efforts are threefold: measuring structure through neural-level image processing, manipulating neural function by using implantable optical methods, and modeling structure and function through neurocomputational control circuits.

In our first effort, we are taking advantage of the recent advances in intact brain imaging developed by the MIT Chung Lab. These advances make it possible to collect volumetric images of brain tissue at cellular resolutions. Together with the MIT Chung Lab, we are developing robust and scalable automated neuron tracing algorithms that will provide the building blocks for developing state-of-the-art brain mapping capabilities. These capabilities will allow us to perform connectivity analysis, such as tracing specific long fibers, computing fiber density and orientations in a local region, and identifying fiber crossings.

In our second effort, we are using a powerful technique called optogenetics to monitor and control the

functioning of populations of neurons in vivo. In collaboration with the MIT Synthetic Neurobiology Group, we are discovering methods of exciting individual neurons at arbitrary sites in the brain in a controllable, single-cell manner. This ability would open the possibility of in vivo analysis of network connectivity at the single-cell level, even in deep brain tissue that is difficult to access. We are developing an electrically controlled, micron-scale liquid lens that provides adjustable focusing and beam steering; the lens will be used for optogenetic in vivo mapping of brain activity with single-cell resolution.

In our third effort, we are applying conventional functional magnetic resonance imaging (fMRI) to modeling perception-action control of sensorimotor activities within the context of neurological disease. With our collaboration with the Gabrieli Laboratory and the Senseable Intelligence Group in the MIT McGovern Institute for Brain Research, we have developed and continue to develop scientifically grounded models through fMRI brain imaging to extract neurocomputationally

inspired biomarkers from speech and potentially other behavioral measurements. These models could improve the detection, monitoring, and phenotyping of neurological disease. We aim to transition this technology to the real world through mobile applications.

## Brain Structure and Function

### Anatomy

The brain is the body's most complex organ, governing motor activity, cognition, and emotion [1]. Figure 1 shows the brain's structure, illustrating the many components that make up its anatomy.

To use a computer analogy, picture the brain as the central processing unit of the body. Processing in the brain is neither exclusively digital nor analog [2]. Information coming into the brain from sensory cues (e.g., speech, audio, pressure, and pain) stimulates neural activity in the brain, with decision making being statistical rather than deterministic [3]. The brain is surrounded by an aqueous layer of cerebrospinal fluid that functions as

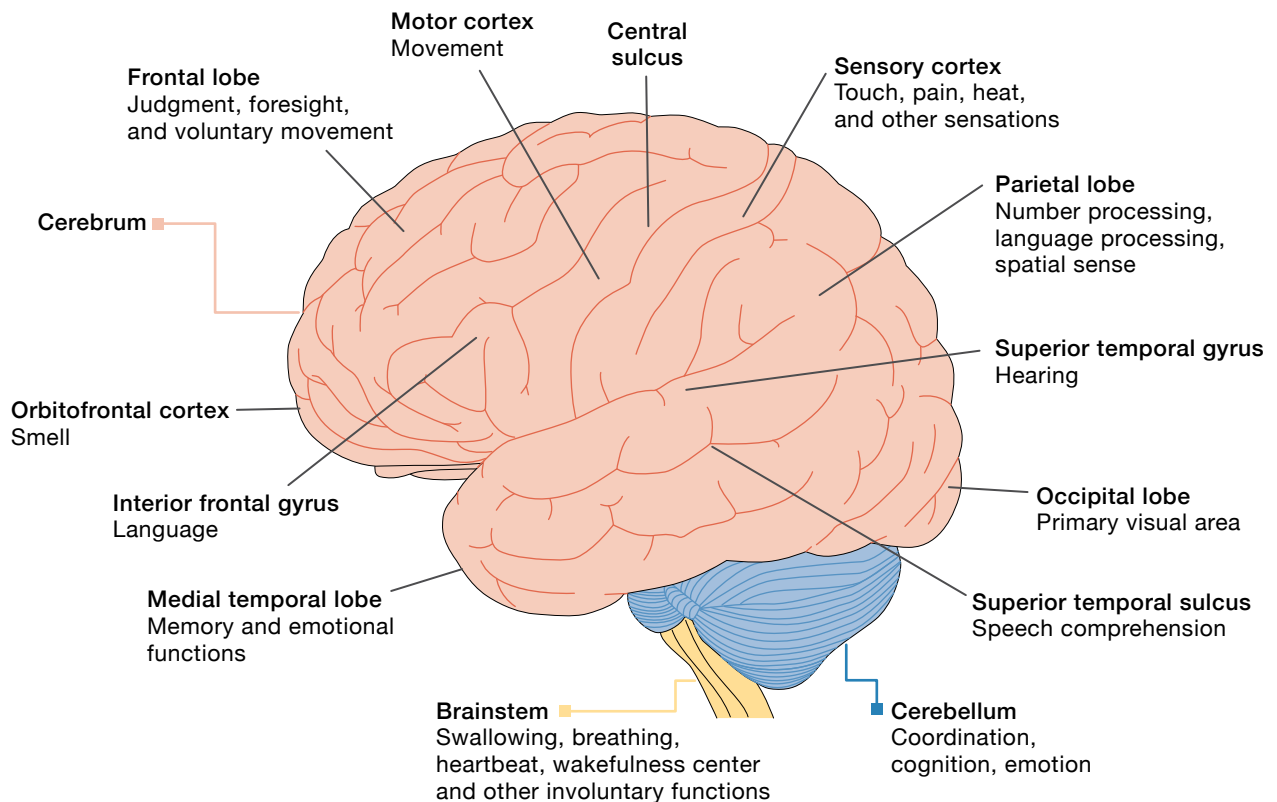


**FIGURE 1.** There are three principal sections of the brain: the cerebrum, cerebellum, and brainstem. Thirteen of the cerebrum's structural regions are shown along with some of their associated functions, though these regions are highly connected and can share responsibilities.

a shock absorber to mitigate trauma when the head is jarred or struck. The gross anatomy of the brain consists of three principal sections: the cerebrum, the cerebellum, and the brainstem. The largest section, occupying about two-thirds of the brain, is the cerebrum. Anatomically, it is divided into two lobes (referred to as the left brain and the right brain) containing the topical cerebral cortex layer and deeper structures, such as the hypothalamus, the olfactory bulbs, and the basal ganglia. The highly invaginated adult cerebral cortex has a surface area of about 2.5 square feet [4]. The cerebellum, occupying the rear section of the brain, is the brain's integration and coordination center, while the brainstem forms the connection with the spinal cord. The adult brain has more than 80 billion neurons along with supporting glial cells, which can be thought of as electrical insulators that prevent "short circuiting" between different neural pathways.

The left and right sides of the brain can each be further divided into four sublobes—frontal, parietal, temporal, and occipital—that play unique roles in information processing. The frontal lobe is the higher cognitive center of the brain, responsible for complex activities, such as problem solving, abstract reasoning, and moral judgment. The parietal lobe integrates sensory information such as touch, taste, and temperature and enables activities like reading and addition. The temporal lobe's central role is auditory perception, but it also plays a significant role in memory. Damage to the right and left temporal lobes has different manifestations. As examples, right-lobe damage impacts drawing and music skills, while left-lobe damage impacts memory and verbal communication. Finally, the occipital lobe is the brain's vision processing center, enabling comprehension of what the eyes are seeing.

### Function and Connectivity

Understanding both anatomical and functional connectivity in the brain is important to all three areas of our brain research. Anatomical connectivity is defined by the physical connections between neurons in the brain and the strength of electrical transmission along these "wired" pathways. These regions of connectivity, called synaptic junctions, occur where the threadlike transmission regions of neurons (axons) interface with branchlike receptors (dendrites) of other neurons in close proximity. Synaptic strength, which is often used as a benchmark of

anatomical connectivity, refers to the amount of current that is passed through a synaptic junction. Interestingly, the brain is continually rewiring itself, a concept often referred to as brain plasticity [5]. Anatomical mapping of the wiring between individual neural paths has shown that strong, persistent synaptic strength, measured on the order of minutes, fades because of the formation and electrical reinforcement of new synaptic junctions, which take hours to days to form [6].

In contrast to anatomical connectivity, functional connectivity can be regarded as an abstraction of the anatomical wiring of the brain. To understand functional connectivity, we look at regions of brain activity (or inactivity) rather than mapping signal transmissions along connected neurons. Techniques such as fMRI are used to map functional connectivity, imaging temporal synchronous activity fluctuations across short- and long-range regions of the brain that can be correlated with activities such as speaking, exercising, and sleeping [7]. Functional maps created from tools like fMRI are largely statistical. They show cross-correlation of activity at both gross resolutions (between different structural areas of the brain) and at millimeter scales (in specific regions like the cerebral cortex).

### Large-Scale Brain Research Accelerator for Interconnected Neurons Microscopy Background

A major goal of the U.S. government's Brain Research through Advancing Innovative Neurotechnologies (BRAIN) Initiative is to map the human brain at different scales with improved speed and accuracy [8]. At the macroscale, significant progress has been made in identifying long-range connectivity of axon bundles using MRI and diffusion tensor imaging [9–11]. At the microscale, electron microscopy (EM) or scanning electron microscopy (SEM) can capture fine details in extremely thin slices of the brain circuitry [12]. Although many semi-automated segmentation techniques have been developed, the processing of EM/SEM images is still limited in throughput by the machinery required to prepare the microslices and the effort required to segment and proof the content of the images [13]. To bridge the gap between macro- and microscale imaging, light-based microscopy provides mesoscale brain imaging with improved throughput [14].

A recent significant advancement in light microscopy is the CLARITY method, which was developed for intact tissue processing [15, 16]. CLARITY (which stands for clear lipid-exchanged acrylamide-hybridized rigid imaging/immunostaining/ in situ-hybridization-compatible tissue hydrogel) removes lipids that cause biological samples to be optically opaque, while preserving molecules of interest, such as proteins. This approach eliminates the need for slicing tissues into micrometer-thick sections and, for example, enables volumetric imaging of an intact mouse brain at a subcellular resolution. A successive technique, magnified analysis of proteome, or MAP [17], further improves the resolution available in intact tissues by physically expanding the tissue fourfold linearly, thus achieving super-resolution as fine as 60 nanometers (nm). This improved resolution enables light microscopy to reveal subcellular structures, such as synaptic components and intercrossing neuronal fibers in the brain.

### Image Processing Approach

Despite the advances in brain imaging at different scales, dense mapping at the cellular resolution of individual neurons and neurites has been hampered by the lack of automated image processing capabilities [18]. Challenges include the large volume of data (e.g., CLARITY microscopy can generate one terabyte per hour), the density of intertwined axons and cells, and the high tracing accuracies required to avoid losing neural connections.

Existing neuron-tracing methods primarily focus on tracing single-neuron morphology [19–24], which typically includes the neural cell body (soma), axon (fiber), and branches (dendrites). A popular open-source biomedical image visualization and analysis software suite is Vaa3D [25, 26], which contains plugins that range from image filtering to neuron tracing. In our experience, we have found that Vaa3D’s most recent

neuron-tracing algorithms, such as Rivulet [27], are mainly designed for tracing a single neuron structure at a time, where all detected foreground pixels are considered connected. This process is different from tracing high-density neuronal fibers, such as those imaged by CLARITY/MAP, in which even closely spaced long-range axonal fibers usually are not connected.

Through Lincoln Laboratory’s Large-Scale Brain Research Accelerator for Interconnected Neurons project, we are collaborating with the MIT Chung Lab to develop a new platform to enable large-scale, long-range fiber-connectivity analysis at resolutions that have not been explored. This effort is supporting the MIT Chung Lab’s Integrated 3D Reconstruction of Whole Human Brains at Subcellular Resolution project, which is working with the Senseable Intelligence Group’s Distributed Archives for Neurophysiology Data Integration project, as part of the BRAIN Initiative Cell Census Network, to generate and disseminate cellular-level data from humans and other species.

Initial progress is presented here on a processing pipeline for automated tracing and connectivity mapping for high-density volumetric neuronal fibers. This is the first reported work to automatically trace densely packed, immunolabeled axonal fibers in CLARITY/MAP data.

To address the unmet gap in large-scale neuron tracing, we developed the following machine learning-based, high-performance computing pipeline (Figure 2):

1. A convolutional neural network detects axon fiber voxels.
2. Morphological operations extract fiber centerlines.
3. Tracking logic connects fiber segments across low-intensity gaps and unresolved fiber crossings.

The pipeline was implemented on a CPU cluster and tested on a 250-gigabyte volume of SMI-312 densely labeled axon fibers, imaged from parts of the hippocampus and cortex of a MAP-processed mouse brain. The pipeline automatically traced 221,298 fibers across

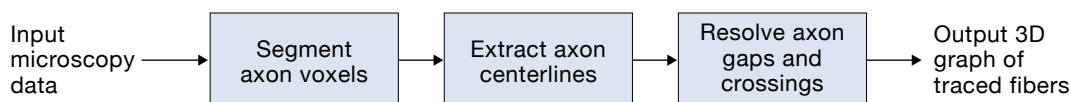


**FIGURE 2.** Microscopy data from mouse brain slices imaged by using MAP are taken as input into the pipeline. Voxels, or clusters of pixels in the image representing brain cells, of axon fibers are segmented, and their centerlines are determined. The system then identifies gaps and crossings between axon fibers and outputs a 3D graph of the axon fibers.

gray and white matter in 10 hours. Of the traced fibers, 104 exceeded 1 millimeter (mm), with the longest being 2.16 mm. The reported accuracy of 84 percent was based on manual evaluation of the 200 longest fibers. An example of neuron tracings is given in Figure 3.

While there is room to improve accuracy, this pipeline offers a significantly faster and more efficient method of tracing neurons than either tracing one neuron at a time or manual fiber tracing. Our pipeline can be a powerful tool for identifying and understanding the subcellular connections in the brain. The sheer number of automatically traced fibers offers a basis for high-level analysis to assess large-scale distribution statistics of long-range fiber connectivity, orientation, length, and diameter. The pipeline allows for new training data

generated from the validated fiber tracings to be fed back into the convolutional neural network model for continuous improvement of system performance. As the pipeline is scaled up to trace axon connections in larger regions of the brain, the connectivity patterns can potentially provide insight into the underlying mechanisms involved with various brain disorders.

### Optogenetics to Control Neural Circuitry Manipulation Background

In the last decade, optogenetics has emerged as a powerful tool to monitor and control the functioning of neuron populations in vivo [28]. Optogenetics involves selectively photoexciting neurons that are genetically modified to express photosensitive membrane proteins (opsins) [29].

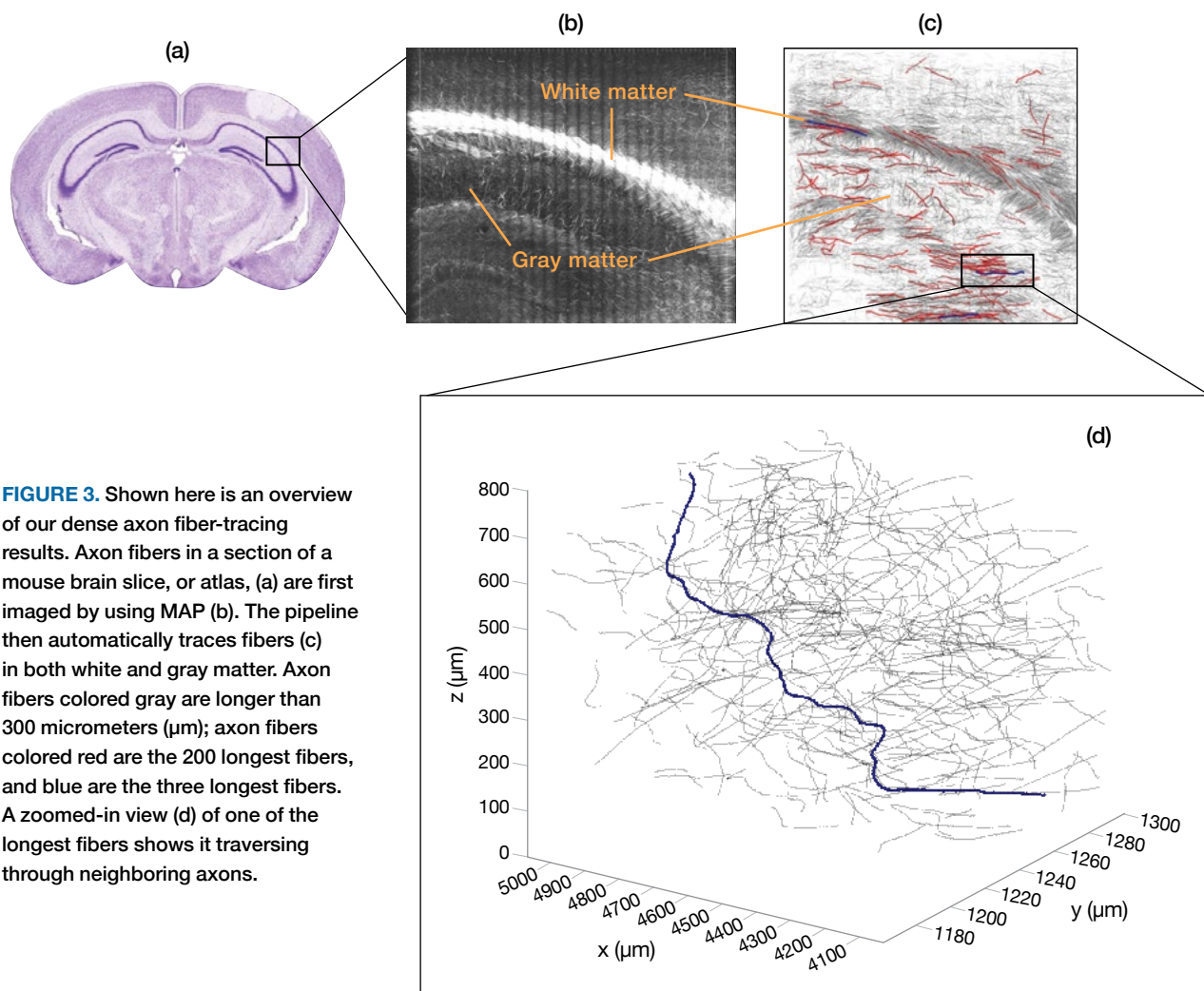


**FIGURE 3.** Shown here is an overview of our dense axon fiber-tracing results. Axon fibers in a section of a mouse brain slice, or atlas, (a) are first imaged by using MAP (b). The pipeline then automatically traces fibers (c) in both white and gray matter. Axon fibers colored gray are longer than 300 micrometers ( $\mu\text{m}$ ); axon fibers colored red are the 200 longest fibers, and blue are the three longest fibers. A zoomed-in view (d) of one of the longest fibers shows it traversing through neighboring axons.

Upon excitation, these opsins transport ions into or out of neurons to control their electrical activity. So far, most optogenetics studies have involved photoexcitation with limited spatial resolution, relying on orthogonal genetically modified channelrhodopsins. These opsins respond to different colors of light that are selectively expressed in different classes of neurons [30]. Two-photon control is possible but only within the shallow depths (i.e., less than 1 mm) afforded by two-photon penetration into the brain [31–33]. Thus, it is highly desirable to have a method of exciting individual neurons at arbitrary sites in the brain in a controllable and single-cell manner because this method would open the possibility of *in vivo* analysis of network connectivity at the single-cell level, even in deep brain tissue that is difficult to access.

Our ultimate goal is to develop an implantable optical probe that has active focusing and steering optics placed at the end of the probe to enable light delivery from an external laser to individual neurons. We have made progress in the first phase of our work, namely engineering micron-scale liquid lenses with active electronics to enable both focusing and steering. These lenses are designed in such a way that, in later phases of the program, they can be integrated with waveguides operating in the red and near-infrared spectra, building from previous work we have done on micro-fabricated waveguide-mediated optogenetic control [34]. This integration will enable two-photon optogenetic excitation of individual cells at arbitrary locations in living mammalian brains.

### Fabrication Approach

We employ optofluidics, whereby microlenses with diameters as small as 50 micrometers ( $\mu\text{m}$ ) are formed by shaping the interface between two immiscible liquids with different refractive indexes. Electrowetting [35] is used to control the shape of the liquid-liquid interface, thus providing variable focus and beam-steering functionalities. With electrowetting, the surface energy of the solid substrate is modified by the application of a voltage, changing it from hydrophobic to hydrophilic in prescribed regions via suitably designed electrodes covered by a hydrophobic film. Previously, Lincoln Laboratory developed liquid, plano-convex, adjustable-focal-length microlenses with electrode diameters as small as 200  $\mu\text{m}$  [36]. In our current work, a novel design of the

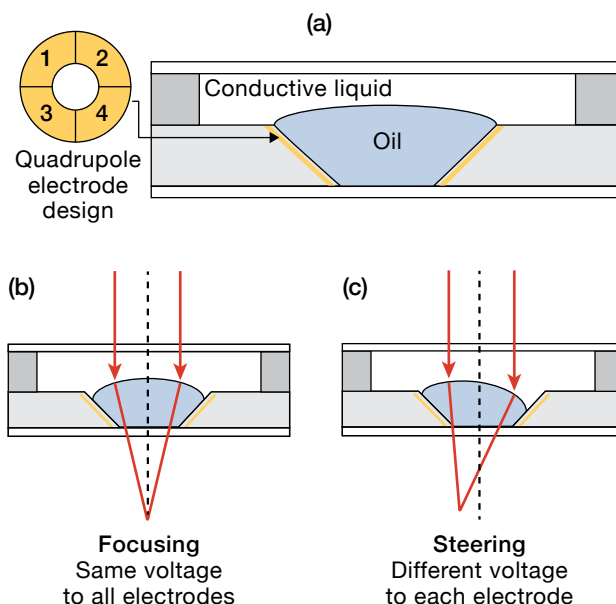


**FIGURE 4.** The liquid microlens design combines both active focusing and beam steering by controlling the interface formed between two immiscible liquids (a). The liquid interface is contained within a 45° conical taper that has a series of patterned metal electrodes etched along the sidewall. Through electrowetting, the interface curvature changes as a function of applied voltage to the electrodes. Variable focusing (b) along the optical path will occur when the same potential is applied to all the electrodes. Beam steering (c) will occur when different potentials are applied to each electrode.

substrate and electrodes has allowed for beam steering and a significant reduction in the microlens diameter.

A target area for excitation that contains 100,000 neuron cell bodies would require a microlens with an adjustable focal length of 0.1–1 mm and simultaneous steering over  $\pm 5$  degrees, and capable of delivering light to a spot size of  $\sim 10 \mu\text{m}$ . To minimize the overall size of the optic, focusing and steering adjustments are made via a single optical element. Both functionalities are achieved by embedding the liquid interface in a conical taper, which has interdigitated electrodes patterned along the sidewall and is etched into a fused silica substrate, as shown in Figure 4. Initial designs used either four independent electrodes or a single electrode around the conical taper. For electrowetting to work, one of the liquids needs to be conductive, typically water, and the other liquid needs to be insulating, typically a nonpolar solvent like oil. The positioning of the oil and water forms the microlens and is controlled by a patterned hydrophobic film over the

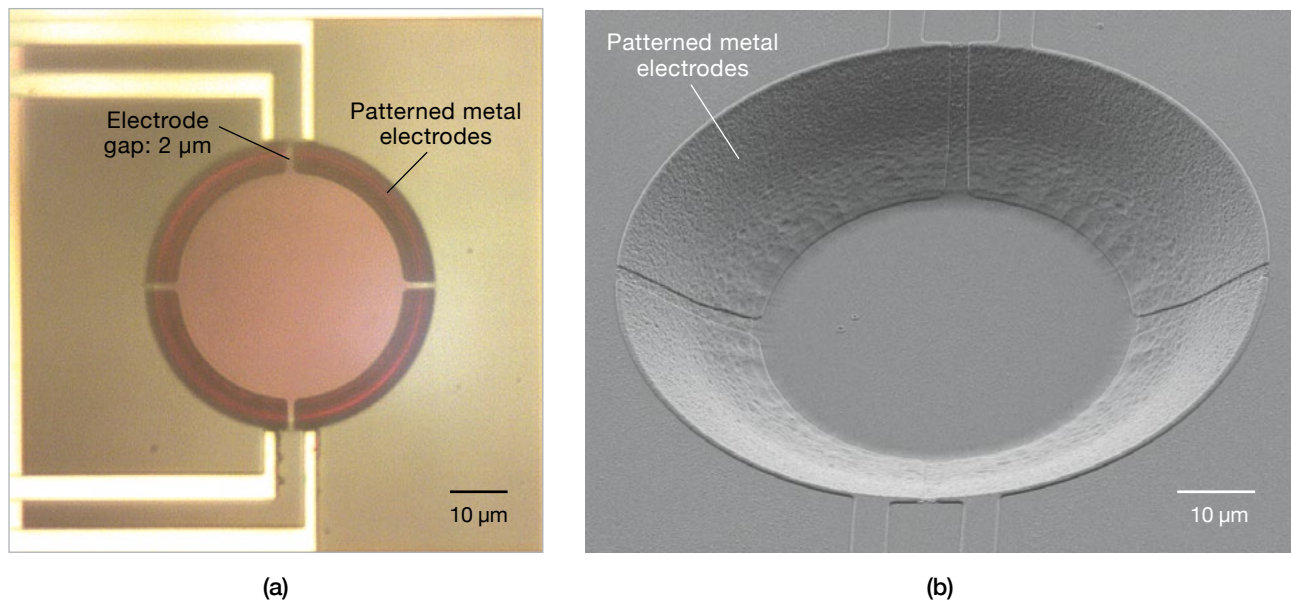


**FIGURE 5.** The top-down microscope image of the microlens cavity (a) shows the electrode metal deposition and patterning. The scanning electron microscopy image (b) was taken after the microlens was fabricated (the CYTOP film had not yet been applied).

electrodes and a surrounding hydrophilic surface. Oil resides inside the taper over the patterned hydrophobic film. When a voltage is applied, the surface energy changes from hydrophobic to more hydrophilic, allowing water to wet over the electrode. This transition changes the radius of curvature of the liquid interface and thus the focal length of the microlens.

The fabricated microlenses have a 12- $\mu\text{m}$ -deep, conical-tapered cavity with a 45-degree sloping sidewall that was etched into a 750  $\mu\text{m}$  fused silica wafer by using a gray-scale lithography technique [37]. A special optical mask designed with subresolution-sized features created a tapered profile in photoresist. The tapered pattern was then transferred into the fused silica through an optimized reaction-ion etching process. Next, 250 nm of aluminum were deposited and etched to form the electrodes. Some microlenses had a quadrupole arrangement. Others had just a single circular electrode, which allows only for adjusting focus in the microlens. After the electrodes were patterned, 500 nm of plasma-enhanced chemical vapor deposition (PECVD) oxide were deposited, forming the dielectric layer. The final fabrication step was to create the hydrophobic and hydrophilic regions. We used 80-nm-thick CYTOP (Asahi Glass) as the hydrophobic film. The film was patterned and etched in oxygen plasma to form hydrophobic regions inside the

taper over the electrodes, leaving hydrophilic regions elsewhere. Figure 5 shows images from the microfabrication process.

To conveniently evaluate the microlens performance, we designed a 10  $\times$  10 mm test chip containing 44 individual microlenses. A completely self-contained microlens package was developed to enable optical characterization. To form the microlenses, the chip was lowered into a beaker containing the conducting liquid with a thin film of oil on the top. Through self-assembly, oil remained on the hydrophobic regions surrounded by the conducting liquid as the chip was lowered into the beaker. While the chip was submerged, a fused silica cap was lowered over it, encapsulating the microlenses. The chip was removed from the beaker, dried, and sealed with epoxy. The sealed chip was wire bonded in a 40-pin dual in-line package, which had a through-hole drilled in the socket region. Finally, the packaged microlens chip was inserted into a zero-insertion-force board-mounted connector to allow for optical characterization.

### Beamforming for Manipulation

To measure the focal length of the liquid microlenses as a function of applied voltage, we developed a novel approach based on beam magnification. The focal length is determined by the change in beam magnification that

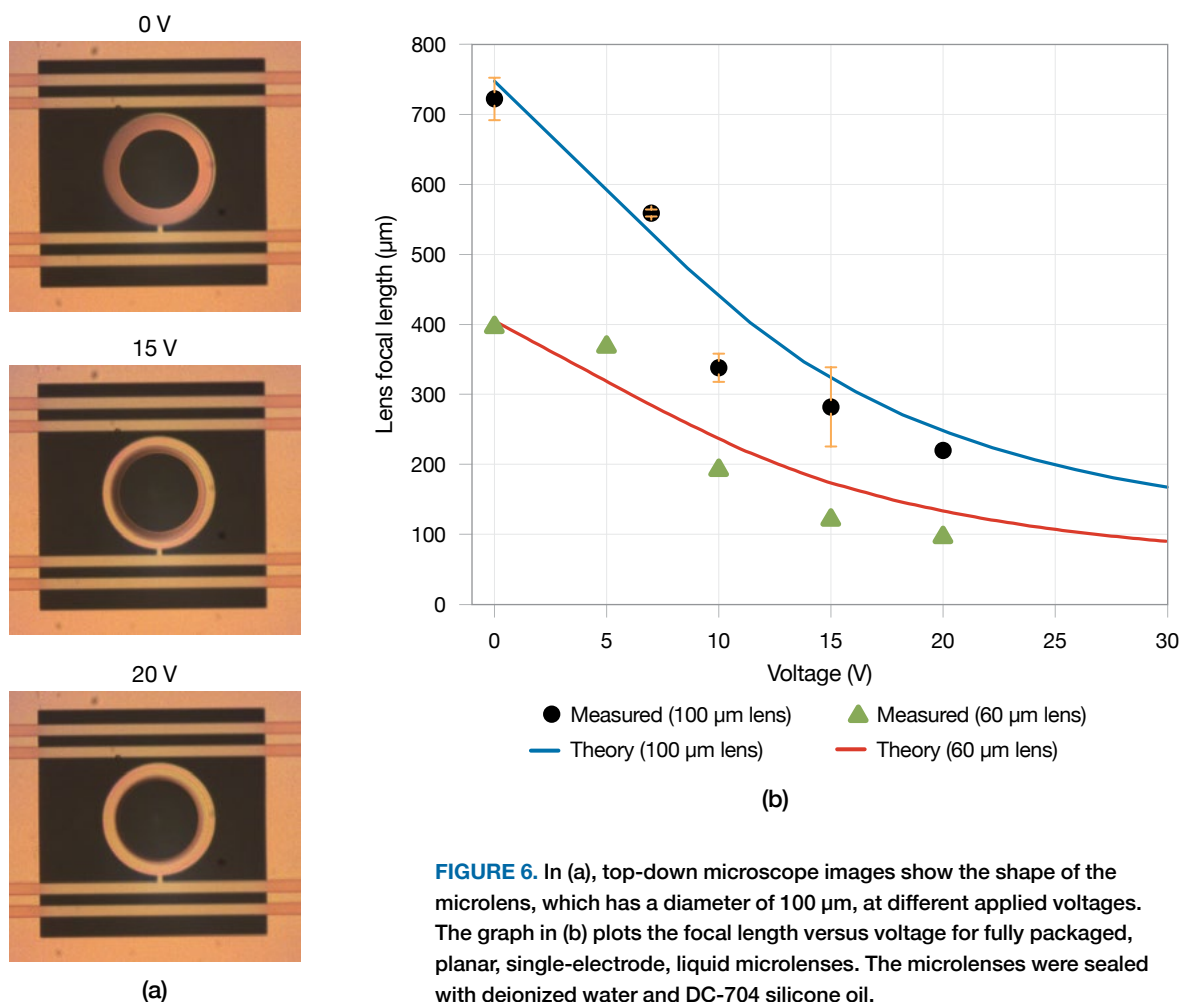


**FIGURE 6.** In (a), top-down microscope images show the shape of the microlens, which has a diameter of 100  $\mu\text{m}$ , at different applied voltages. The graph in (b) plots the focal length versus voltage for fully packaged, planar, single-electrode, liquid microlenses. The microlenses were sealed with deionized water and DC-704 silicone oil.

the microlens imparts on a predetermined beam magnification optical system. The optical diagnostic system focuses a diagnostic beam through the test microlens with an  $\sim 16 \mu\text{m}$  spot size and outputs a beam with a size compatible with a beam-profiling camera. In principle, if the microlens is aligned precisely in the optical diagnostic system, then its focal length can be determined directly from the measured beam size. However, determining the microlens' focal length is difficult in practice. Consequently, the microlens was also translated along the optical axis of the diagnostic system, similar to a z-scan, with beam size measurements recorded at multiple positions. These additional measurements provide sufficient data to relax the alignment tolerance of the microlens, while improving the sensitivity of the focal length measurement. Initial characterization was done by using a helium–neon laser (633 nm wavelength). The microlens focal length was determined by fitting the

measured beam size as a function of translated distance to an exact analytical expression.

Figure 6 shows the focal-length-versus-voltage results from characterizing two fully packaged, planar, single-electrode, liquid microlenses of different sizes. As the voltage is increased, each lens becomes more convex as water wets the electrodes and forces the oil into the center of the aperture, decreasing the effective focal length. Through active control of the focal length, the lenses can be ultimately steered to focus light on individual neurons at different depths in the brain.

### Neurocomputational Modeling Modeling Background

Neurocomputational modeling is the science of constructing and using mathematical models of neurobiophysical processes to characterize brain function [38]. The current standard of care in neuropsychiatry

has not caught up with the wealth of neuroscientific data that new imaging and manipulation techniques have made available. There is a pressing need for a unified, actionable framework for knowledge that is mined from state-of-the-art imaging techniques and ubiquitous data collection technologies, such as smartphones. The challenges are numerous: data are sparse, multimodal, and noisy, and the underlying sensorimotor and cognitive processes at work are seemingly impenetrable in their complexity. Appropriate modeling strategies can address these challenges and have demonstrated potential on real-world data.

Modeling can be divided into two stages: model construction and model use. In model construction, a mathematical summary of relationships between quantitative data is created. Quantitative data are aggregated from subjects under study (e.g., people with Alzheimer's disease, dementia, traumatic brain injury, autism, depression, or Parkinson's disease) and can include modalities such as voice, structural and functional MRI, accelerometer gait data, and known medications. These data are fused with prior knowledge of neuroanatomical function based on previous human and animal studies. Often, a complete prior model does not exist for the data and disorder under study, so model construction also involves a knowledge-discovery component. Modelers must choose between competing possible hypotheses by using their prior knowledge or tools such as Bayesian information criterion and out-of-sample prediction.

Model use is the leveraging of an individual's fitted model to understand and provide treatment for that individual. Models can be used to predict brain responses (e.g., dynamic causal modeling), effectiveness when sleep deprived (e.g., the Sleep, Activity, Fatigue, and Task Effectiveness [SAFTE] model), treatment response (e.g., how neural circuits can be advantageously altered in Parkinson's disease through deep brain stimulation), and neurotraumatic damage. Models also are a compact summary of the subject's data. Consequently, differences between individual models can be used for disease severity assessment and trajectory prediction. The mathematical constants that parameterize a model, whether those are time constants of neural processes or strength and prevalence of functional connectivity, are all potential features for classical machine learning algorithms. Machine learning algorithms trained on these parameters can then

predict responses potentially better than or complementary to those trained on the raw data.

Neurocomputational modeling seeks a mathematical, mechanistic explanation for behavior through the use of observations and hypothesized biophysical and neurological mechanisms. An example of this framework in action is a unifying paradigm of motor control that can be illustrated with a specific example of speech production and the neurological disorders of depression and Parkinson's disease. Our modeling allows a complementary approach to traditional feature engineering schemes, with model features reflecting internal or latent model parameters. This approach is a step toward a brain basis for biomarkers of a disease and thus toward increased clinical acceptance of behavior-based automatic assessment systems [38].

### Imaging as a Modeling Basis

Brain imaging can reveal neurophysiological structures that are relevant for speech, and these structures act as a starting point for neurocomputational models of speech production. Speech production results from the coordinated activity of a distributed set of neuroanatomical regions, as has been determined through various forms of brain imaging. Figure 7 shows examples of fMRI images of some primary regions of the speech network. These regions, determined through speech-production-task studies [39], include cortical and subcortical components as well as the cerebellum and brainstem, and involve feedforward and feedback mechanisms in prosodic, articulatory, and linguistic components of speech production.

Specifically, the posterior superior temporal gyrus and Heschl's gyrus are part of the auditory cortex and are crucial for self-monitoring in speech production feedback. The subcortical basal ganglia (composed in part by the striatum) and the midline cortical areas of the supplementary motor area and presupplementary motor area are responsible for initiation and plan selection and speech sequencing. The motor cortex, specifically the ventral motor cortex, and parts of the inferior frontal gyrus (Broca's area) control the articulators for the actual production of speech. The cerebellum further assists in the fine timing control of articulators needed for well-formed sounds. Prosodic modulation relies on the core speech network but also recruits part

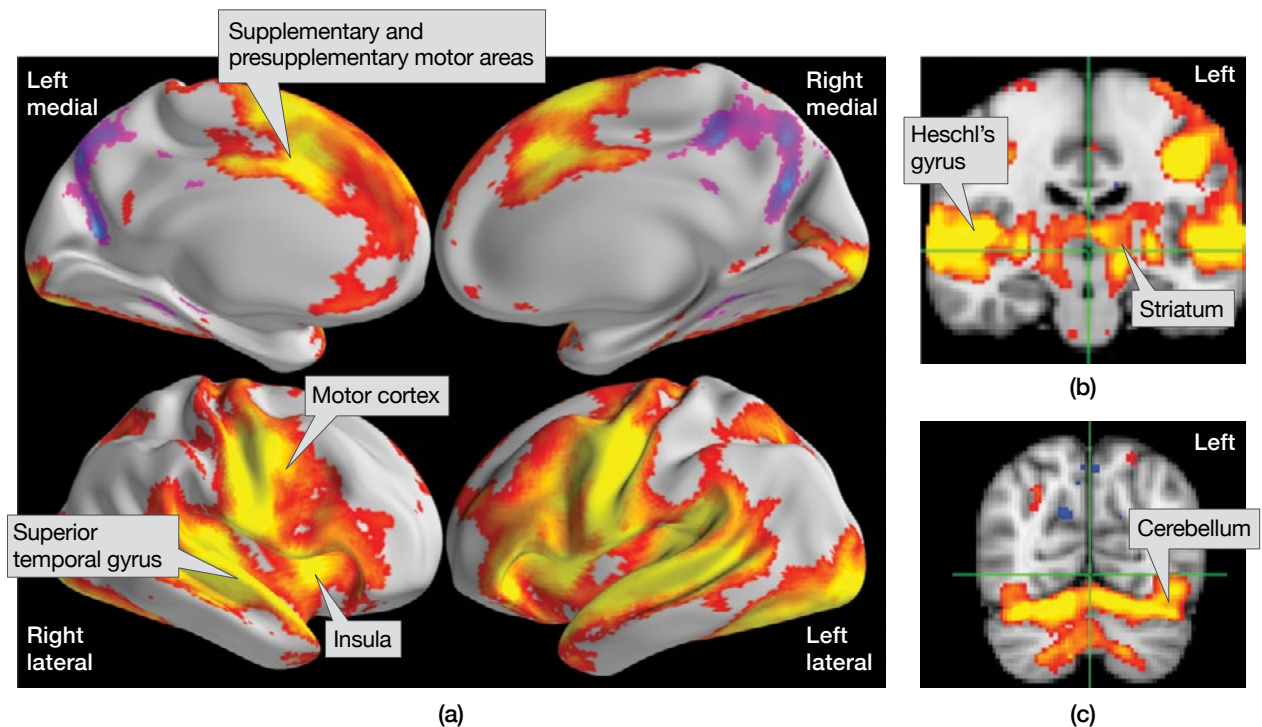


**FIGURE 7.** These functional magnetic resonance images show speech production–related regions of interest in the brain. The four images in (a) show activity in the cortex. The medial views of the brain at top (a) show the supplementary motor area and presupplementary motor area used for speech planning and sequencing. At bottom (a), a lateral view of the brain shows bilateral activation of the motor cortex used for controlling the articulators of speech production and shows the superior temporal gyrus, part of the auditory cortex, used for self-monitoring speech production. The coronal view (b) of the brain shows Heschl’s gyrus, which is involved in auditory processing, and the striatum, which with the insula is hypothesized to connect limbic processing to the speech production system. The coronal view (c) of the posterior brain shows bilateral activation in the cerebellum. The cerebellum assists in precisely timing motor commands in speech production [42].

of the limbic system (e.g., the amygdala and the insula) in emotional speech. F.H. Guenther [39], C.J. Price [40], and S. Pichon et al. [41] provide further details on the neuroanatomy of speech production.

Some of these speech regions overlap or are connected with neuroanatomical regions, such as the amygdala or motor regions, that are associated with our example conditions of depression and Parkinson’s disease, respectively. Details of these links are out of the scope of this article (please see the article “Noninvasive Biomarkers of Neurobehavioral Performance” on page 28 in this *Journal*), but essentially these connections may provide an opportunity for nonspeech processes to influence speech production. The hypothesized modulation of the speech network by nonspeech processes and deficits that can occur in modules of the speech production network provide the guiding motivation for why

speech can be a biomarker of neuropsychological disorders in general and of depression and Parkinson’s disease in particular.

Although not a focus of this article, Lincoln Laboratory’s Human Health and Performance Systems Group is developing mechanism-based modeling approaches to enhance neurotrauma assessments. Imaging is also useful as a structural input to establish neurophysiological-based models, as well as for bioelectric and biomechanical constitutive models of the various hard and soft tissues and fluids that compose brain structures. Energetic impulses can deliver direct traumatic insults to the brain and can be converted to other forms of damaging input (e.g., electromagnetic energy to thermomechanical force) [43]. The time- and temperature-dependent nature of the damaging inputs and the pathophysiological response within the brain

require these neurotrauma models to be based not solely on linear properties [44]. Nonlinear constitutive models (e.g., viscoelasticity, hyperelasticity, and poroelasticity) have been used for high-fidelity damage assessments from photothermal, thermomechanical, and overpressure loads [45]. Our models can input multiple two-dimensional MRI scans to create a three-dimensional neurostructural model with varying nonlinear material properties for ventricles, glia, white matter, gray matter, eyes, venous sinus, cerebrospinal fluid, air sinus, muscle, skin, fat, and trabecular bone (e.g., cranium) [46].

### Perception-Action Framework

Brain imaging representations of the type shown in Figure 7 have motivated neurocomputational models of motor control [39]. A unifying paradigm of motor control is the perception-action framework diagrammed in Figure 8 [47]. We describe a neurophysiological system through several broad components and relationships. The first component is the biophysical plant, or motor system, that is controlled by the controller module, the second component. The third component is a sensing module responsible for perception, and the fourth component is the goal, or plan, responsible for the desired action. While precise delineation of roles is debatable, we will determine for this article that the sensory system detects the state of the plant, and that this current state and the goal—the desired state of the plant as instructed by higher-level cognitive control—are both inputs to the controller. We note that the goal of the system may have a different parameterization than the plant itself has. For example, in speech production the goal may be an auditory target, but the plant configuration that corresponds to such a goal could be specified as a function of articulator positions. The controller then implements corrective action by taking the error between the desired and perceived states and sends a control signal to the biophysical plant. The controller closes the loop between perception and action.

Importantly, the perception-action framework has an “observable biomarker” analog pictured in Figure 9. Although we cannot generally see the workings of the system under study, we can observe various biomarkers that can be used to tune a model of the plant to an approximate match of the real state. Therefore, we use observable biomarkers to provide system identification on what, without a modeling framework, would be a black box.

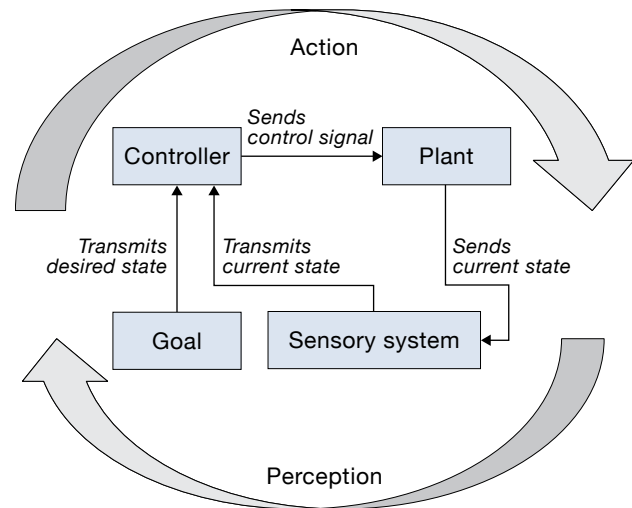


**FIGURE 8.** A neurocomputational modeling framework is based on the perception-action loop, which allows the brain to seamlessly integrate goals, sensory perceptions, and new motor commands to control the plant (i.e., the body) [47].

### Applying Neurocomputational Modeling to Assessing Neuropsychological Disorders

In research by Ciccarelli et al., neurocomputational modeling was implemented with respect to speech motor control and the neurological conditions of depression and Parkinson’s disease [42, 48, 49]. Speech is one of the most complex and demanding motor tasks and draws upon a significant amount of neural “real estate” in the brain. Consequently, speech production biomarkers may be sensitive to neurological disorders. A computational model of speech production that follows the described perception-action paradigm is the Directions into Velocities of Articulators (DIVA) model developed by Guenther et al. [39, 50]. This model describes the workings of the vocal tract resonances that are responsible for creating the acoustic cues that differentiate vowel sounds.

Ciccarelli et al. adopted this particular perception-action framework to describe the vocal folds that are responsible for creating fundamental frequency, which is perceived as pitch [49]. This adoption required leveraging a biophysical model of the vocal folds for the plant, with the vocal source model characterized by two latent muscle parameters, the cricothyroid (CT) and thyroarytenoid (TA) muscles of the larynx. The coordination of the two estimated muscle intensities over time was then used to characterize a disease, with coordination

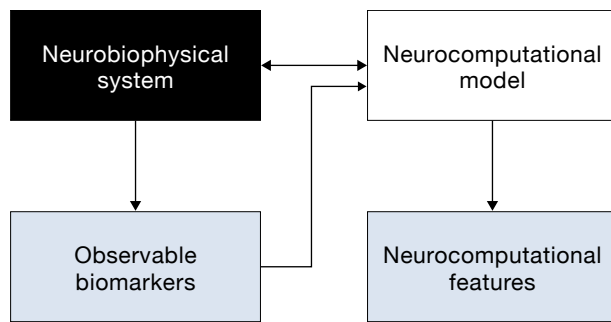


**FIGURE 9.** The black box neurobiophysical system can be investigated with a white box neurocomputational model by estimating model parameters and structure from observable biomarkers. The model can then be used to derive neurocomputational features such as muscle intensities and error signals [49].

represented by multiscale correlation of the CT and TA time series [49, 53]. Ciccarelli et al. embedded this plant representation within the perception-action framework to perform system identification (i.e., the unknown CT and TA muscle intensities) on individuals with depression and Parkinson’s disease [49]. The underlying features estimated in this way were then used as biomarkers to assess the presence or severity of the underlying disorder.

## Results and Discussion

Ciccarelli et al. [49] applied these features to the depression database of the Audio/Visual Emotion Challenge [51], a competition that tasks participants with estimating the level of subjects’ depression by using audio and visual data. Compared to traditional, non-biophysically motivated features, the neurocomputational biophysical features provided nearly twice the explanatory power for depression. Ciccarelli et al. also applied this technique to predicting the severity of Parkinson’s disease by using the mPower database [52], a collection of health-condition data and symptom-progression data from Parkinson’s disease patients. They found that although the model-based features alone underperformed more traditional features, fusion of the two predictors performed better than either alone.

A similar neurocomputational modeling-based approach was also introduced by Ciccarelli [42] and Williamson et al. [48] for vocal tract movement. This approach illustrated the coordination over time of the

vocal tract muscle intensities (responsible for coordinating vocal tract resonances) used to characterize Parkinson’s disease. Again, fusing the model-based features with traditional features provided more benefit than either feature set alone in prediction of severity of Parkinson’s disease [48].

In summary, we advocate a neurobiophysical model embedded within a perception-action framework. A mathematical, mechanistic description of a person can provide new biomarkers through system identification and permit experimental manipulations via computer simulation to potentially provide further insight into neuropsychological disorders, such as depression, Parkinson’s disease, traumatic brain injury, Alzheimer’s disease, and dementia. Such modeling may lead to more accurate and early detection of a neurological disorder, phenotyping of the disorder, monitoring of treatment effects, and predictions of new therapy outcomes.

## Synergy Moving Forward

We have described three areas of brain-related research at Lincoln Laboratory in collaboration with MIT campus: measuring structure through neural-level image processing, manipulating neural function by using implantable optical methods, and modeling structure and function through neurocomputational control circuits.

Though these three efforts may appear disjointed, they are potentially strongly synergistic. Accurate neurocomputational models will rely on more highly resolved connectivity maps obtained through refined neural tracing, while increased understanding of the function of feedforward and feedback model pathways will rely on the manipulation of neural circuits through more advanced optogenetic-based techniques. We believe this synergy will lead to an improved neural mechanistic explanation for behavior and, in particular, improved phenotyping across and within neurological disorders. ■

## References

1. L. Pessoa, “The Cognitive-Emotional Brain: From Interactions to Integration,” *Neuropsychologia*, vol. 48, no. 12, 2010, pp. 3416–3429.
2. Y. Mochizuki and S. Shinomoto, “Analog and Digital Codes in the Brain,” *Physical Review E*, vol. 89, no. 2, 2014, article no. 022705.
3. J.I. Sanders, B. Hangya, and A. Kepecs, “Signatures of a Statistical Computation in the Human Sense of Confidence,” *Neuron*, vol. 90, no. 3, 2016, pp. 499–506.

4. A. Peters and E.G. Jones (eds.), *Cerebral Cortex. Vol 1, Cellular Components of the Cerebral Cortex*. New York: Plenum Press, 1984.
5. H. Johansen-Berg, "Structural Plasticity: Rewiring the Brain," *Current Biology*, vol. 17, no. 4, 2007, pp. R141–R144.
6. L.C. Katz and C.J. Shatz, "Synaptic Activity and the Construction of Cortical Circuits," *Science*, vol. 274, no. 5290, 1996, pp. 1133–1138.
7. N. Kriegeskorte, R. Goebel, and P. Bandettini, "Information-Based Functional Brain Mapping," paper in *Proceedings of the National Academy of Sciences of the United States of America*, vol. 103, no. 10, 2006, pp. 3863–3868.
8. "Brain Research through Advancing Innovative Neurotechnologies (BRAIN) —National Institutes of Health (NIH)," available at <https://www.braininitiative.nih.gov/>.
9. O. Sporns, "The Human Connectome: a Complex Network," *Annals of the New York Academy of Science*, vol. 1224, no. 1, 2011, pp. 109–125.
10. A. Zalesky, A. Fornito, I.H. Harding, L. Cocchi, M. Yücel, C. Pantelis, et al., "Whole-Brain Anatomical Networks: Does the Choice of Nodes Matter?" *NeuroImage*, vol. 50, no. 3, 2010, pp. 970–983.
11. J.C. Shillcock, M. Hawrylycz, S. Hill, and H. Peng, "Reconstructing the Brain: From Image Stacks to Neuron Synthesis," *Brain Informatics*, vol. 3, no. 4, 2016, pp. 205–209.
12. M. Helmstaedter, K.L. Briggman, S.C. Turaga, V. Jain, H.S. Seung, and W. Denk, "Connectomic Reconstruction of the Inner Plexiform Layer in the Mouse Retina," *Nature*, vol. 500, no. 7461, 2013, pp. 168–174.
13. I. Arganda-Carreras, S.C. Turaga, D.R. Berger, D. Cireşan, A. Giusti, L.M. Gambardella, et al., "Crowdsourcing the Creation of Image Segmentation Algorithms for Connectomics," *Frontiers in Neuroanatomy*, vol. 9, 2015, p. 142.
14. M.B. Ahrens, M.B. Orger, D.N. Robson, J.M. Li, and P.J. Keller, "Whole-Brain Functional Imaging at Cellular Resolution Using Light-Sheet Microscopy," *Nature Methods*, vol. 10, no. 5, 2013, pp. 413–420.
15. K. Chung and K. Deisseroth, "CLARITY for Mapping the Nervous System," *Nature Methods*, vol. 10, no. 6, 2013, pp. 508–513.
16. K. Chung, J. Wallace, S.-Y. Kim, S. Kalyanasundaram, A.S. Andalman, T.J. Davidson, et al., "Structural and Molecular Interrogation of Intact Biological Systems," *Nature*, vol. 497, no. 7449, 2013, pp. 332–337.
17. T. Ku, J. Swaney, J.-Y. Park, A. Albanese, E. Murray, J.H. Cho, et al., "Multiplexed and Scalable Super-Resolution Imaging of Three-Dimensional Protein Localization in Size-Adjustable Tissues," *Nature Biotechnology*, vol. 34, no. 9, 2016, pp. 973–981.
18. J.W. Lichtman, H. Pfister, and N. Shavit, "The Big Data Challenges of Connectomics," *Nature Neuroscience*, vol. 17, no. 11, 2014, pp. 1448–1454.
19. Y. Wang, A. Narayanaswamy, C.-L. Tsai, and B. Roysam, "A Broadly Applicable 3-D Neuron Tracing Method Based on Open-Curve Snake," *Neuroinformatics*, vol. 9, no. 2–3, 2011, pp. 193–217.
20. E. Türetken, G. González, C. Blum, and P. Fua, "Automated Reconstruction of Dendritic and Axonal Trees by Global Optimization with Geometric Priors," *Neuroinformatics*, vol. 9, no. 2–3, 2011, pp. 279–302.
21. P. Chothani, V. Mehta, and A. Stepanyants, "Automated Tracing of Neurites from Light Microscopy Stacks of Images," *Neuroinformatics*, vol. 9, no. 2–3, 2011, pp. 263–278.
22. H. Peng, F. Long, and G. Myers, "Automatic 3D Neuron Tracing Using All-Path Pruning," *Bioinformatics*, vol. 27, no. 13, 2011, pp. i239–i247.
23. E. Bas and D. Erdogmus, "Principal Curves as Skeletons of Tubular Objects," *Neuroinformatics*, vol. 9, no. 2–3, 2011, pp. 181–191.
24. M.H. Longair, D.A. Baker, and J.D. Armstrong, "Simple Neurite Tracer: Open Source Software for Reconstruction, Visualization and Analysis of Neuronal Processes," *Bioinformatics*, vol. 27, no. 17, 2011, pp. 2453–2454.
25. H. Peng, Z. Ruan, F. Long, J.H. Simpson, and E. W. Myers, "V3D Enables Real-Time 3D Visualization and Quantitative Analysis of Large-Scale Biological Image Data Sets," *Nature Biotechnology*, vol. 28, no. 4, 2010, pp. 348–353.
26. H. Peng, A. Bria, Z. Zhou, G. Iannello, and F. Long, "Extensible Visualization and Analysis for Multidimensional Images Using Vaa3D," *Nature Protocols*, vol. 9, no. 1, 2014, pp. 193–208.
27. S. Liu, D. Zhang, S. Liu, D. Feng, H. Peng, and W. Cai, "Rivulet: 3D Neuron Morphology Tracing with Iterative Back-Tracking," *Neuroinformatics*, vol. 14, no. 4, 2016, pp. 387–401.
28. K. Deisseroth, G. Feng, A. Majewska, G. Miesenbröck, A. Ting, and M. Schnitzer, "Next-Generation Optical Technologies for Illuminating Genetically Targeted Brain Circuits," *Journal of Neuroscience*, vol. 26, no. 41, 2006, p. 10380.
29. E. Boyden, F. Zhang, E. Bamberg, G. Nagel, and K. Deisseroth, "Millisecond-Timescale, Genetically Targeted Optical Control of Neural Activity," *Nature Neuroscience*, vol. 8, no. 9, 2005, pp. 1263–1268.
30. N.C. Klapoetke, Y. Murata, S.S. Kim, S.R. Pulver, A. Birdsey-Benson, Y.K. Cho, et al., "Independent Optical Excitation of Distinct Neural Populations," *Nature Methods* vol. 11, 2014, pp. 338–346.
31. J.P. Rickgauer, and D.W. Tank, "Two-Photon Excitation of Channelrhodopsin-2 at Saturation," paper in *Proceedings of the National Academy of Sciences of the United States of America*, vol. 106, no. 35, 2009, pp. 15025–15030.
32. B.K. Andrasfalvy, B.V. Zelman, J. Tang, and A. Vaziri, "Two-Photon Single-Cell Optogenetic Control of Neuronal Activity by Sculpted Light," paper in *Proceedings of the National Academy of Sciences of the United States of America*, vol. 107, no. 26, 2010, pp. 11981–11986.

33. E. Papagiakoumou, F. Anselmi, A. Bègue, V. de Sars, J. Glücksta, E.Y. Isacoff, and V. Emiliani, "Scanless Two-Photon Excitation of Channelrhodopsin-2," *Nature Methods*, vol. 7, no. 10, 2010, pp. 848–854.
34. A.N. Zorzos, J. Scholvin, E.S. Boyden, and C.G. Fonstad, "Three-Dimensional Multiwaveguide Probe Array for Light Delivery to Distributed Brain Circuits," *Optics Letters*, vol. 37, no. 23, 2012, pp. 4841–4843.
35. F. Mugele and J.-C. Baret, "Electrowetting: From Basics to Applications," *Journal of Physics: Condensed Matter*, vol. 17, no. 28, 2005, pp. R705–R774.
36. S. Berry, J. Stewart, T. Thorsen, and I. Guha, "Development of Adaptive Liquid Microlenses and Microlens Arrays," paper in MOEMS and Miniaturized Systems XII, *Proceedings of SPIE*, vol. 8616, 2013, pp. 861610–8616101.
37. C.M. Waits, R. Ghodssi, M.H. Ervin, and M. Dubey, "MEMS-Based Gray-Scale Lithography," paper in *2001 International Semiconductor Device Research Symposium Proceedings*, 2001, pp. 182–185.
38. T.V. Wiecki, J. Poland, and M.J. Frank, "Model-Based Cognitive Neuroscience Approaches to Computational Psychiatry Clustering and Classification," *Clinical Psychological Science*, vol. 3, no. 3, 2015, pp. 378–399.
39. F.H. Guenther, *Neural Control of Speech*. Cambridge, Mass.: MIT Press, 2016.
40. C.J. Price, "A Review and Synthesis of the First 20 years of PET and fMRI Studies of Heard Speech, Spoken Language and Reading," *NeuroImage*, vol. 62, no. 2, 2012, pp. 816–847.
41. S. Pichon and C.A. Kell, "Affective and Sensorimotor Components of Emotional Prosody Generation," *Journal of Neuroscience*, vol. 33, no. 4, 2013, pp. 1640–1650.
42. G. Ciccarelli, "Characterization of Phoneme Rate as a Vocal Biomarker of Depression," Dissertation, MIT, 2017.
43. N.M. Yitzhak, R. Ruppin, and R. Hareuveny, "Numerical Simulation of Pressure Waves in the Cochlea Induced by a Microwave Pulse," *Bioelectromagnetics*, vol. 35, no. 7, 2014, pp. 491–496.
44. T.P. Prevost, A. Balakrishnan, S. Suresh, and S. Socrate, "Biomechanics of Brain Tissue," *Acta Biomaterialia*, vol. 7, no. 1, 2011, pp. 83–95.
45. D.F. Moore, A. Jérusalem, M. Nyein, L. Noels, M.S. Jaffee, and R.A. Radovitzky, "Computational Biology—Modeling of Primary Blast Effects on the Central Nervous System," *NeuroImage*, vol. 47, 2009, pp. T10–T20.
46. A. Jeana, M.K. Nyeina, J.Q. Zheng, D.F. Moore, J.D. Joannopoulos, and R. Radovitzky, "An Animal-to-Human Scaling Law for Blast-Induced Traumatic Brain Injury Risk Assessment," paper in *Proceedings of the National Academy of Sciences of the United States of America*, vol. 111, no. 43, 2014, pp. 15310–15315.
47. V. Cutsuridis, A. Hussain, and J.G. Taylor, *Perception-Action Cycle: Models, Architectures, and Hardware*. New York: Springer, 2011.
48. J.R. Williamson, T.F. Quatieri, B.S. Helfer, J. Perricone, S.S. Ghosh, G. Ciccarelli, and D.D. Mehta, "Segment-Dependent Dynamics in Predicting Parkinson's Disease," paper presented at INTERSPEECH 2015: 16th Annual Conference of the International Speech Communication Association, 2015.
49. G.A. Ciccarelli, T.F. Quatieri, and S.S. Ghosh, "Neurophysiological Vocal Source Modeling for Biomarkers of Disease," paper in *Proceedings of INTERSPEECH 2016: Understanding Speech Processing in Humans and Machines*, 2016, pp. 1200–1204.
50. F.H. Guenther, S.S. Ghosh, and J.A. Tourville, "Neural Modeling and Imaging of the Cortical Interactions Underlying Syllable Production," *Brain and Language*, vol. 96, no. 3, 2006, pp. 280–301.
51. M. Valstar, B. Schuller, K. Smith, F. Eyben, B. Jiang, S. Bilakhia, et al., "AVEC 2013: The Continuous Audio/Visual Emotion and Depression Recognition Challenge," paper in *Proceedings of the 3rd ACM International Workshop on Audio/Visual Emotion Challenge*, 2013, pp. 3–10.
52. B.M. Bot, C. Suver, E.C. Neto, M. Kellen, A. Klein, C. Bare, et al., "The mPower Study, Parkinson Disease Mobile Data Collected Using ResearchKit," *Scientific Data*, vol. 3, 2016, article no. 160011.
53. J.R. Williamson, D.W. Bliss, D.W. Browne, and J.T. Narayanan, "Seizure Prediction Using EEG Spatiotemporal Correlation Structure," *Epilepsy & Behavior*, vol. 25, no. 2, 2012, pp. 230–238.

#### About the Authors



Thomas F. Quatieri, a senior member of the technical staff in the Human Health and Performance Systems Group, is involved in bridging human language and bioengineering research and technologies. Within this group, he has initiated and developed major R&D and technology transition programs in speech

and auditory signal processing and neuro-biophysical modeling with application to detection and monitoring of neurological, neurotraumatic, and stress conditions. He has been an author on more than 200 publications, holds 11 patents, and authored the textbook *Discrete-Time Speech Signal Processing: Principles and Practice*. He also holds a faculty appointment in the Harvard-MIT Speech and Hearing Bioscience and Technology Program. He developed the MIT graduate course Digital Speech Processing and is active in advising graduate students on the MIT and Harvard campuses. He is a recipient of four IEEE Transactions Best Paper Awards and the 2010 MIT Lincoln Laboratory Best Paper Award. He led the Lincoln Laboratory team that won the 2013 and 2014 AVEC Depression Challenges and the 2015 MIT Lincoln Laboratory Team Award for their work on vocal and facial biomarkers. He has served on the IEEE Digital Signal Processing Technical Committee, the IEEE Speech and Language Technical Committee, and the IEEE James L. Flanagan Speech and Audio Awards Committee. He has served on National Institutes of Health and National Science Foundation

panels, been an associate editor for the *IEEE Transactions on Signal Processing*, and is an associate editor of *Computer, Speech, and Language*. He has been an invited speaker at conferences, workshops, and meetings, most recently as a keynote speaker at the 2019 Speech Science and Technology Conference. He is a Fellow of the IEEE and a member of Tau Beta Pi, Eta Kappa Nu, Sigma Xi, International Speech and Communication Association, Society for Neuroscience, Association for Research in Otolaryngology, and the Acoustical Society of America. He holds a bachelor's degree (summa cum laude) from Tufts University, and master's, electrical engineering, and doctoral degrees from MIT.



**Laura J. Brattain** works at the intersection of biomedical image processing, artificial intelligence, high-performance computing, and biorobotics. She is a technical staff member in the Human Health and Performance Systems Group and the principal investigator of a number of biomedical image

processing programs. She collaborates closely with MIT campus and Boston-area hospitals, including Massachusetts General Hospital. She holds a doctoral degree in bioengineering from Harvard University.



**Todd A. Thorsen** is a technical staff member in the Biological and Chemical Technologies Group, where he pursues research in microfluidics-based engineering, including the design and fabrication of state-of-the-art programmable microfluidic devices, exploitation of the microscale physical properties

of fluids (thermal, chemical, optical, and electrical), and the development of microfluidic platforms for medicine. Prior to joining Lincoln Laboratory, he was a faculty member in the MIT Department of Mechanical Engineering. He has authored or coauthored 34 papers and two book chapters, has 40 issued and pending patents in the field of microfluidics, and has more than 8,800 citations of his published works. He holds a bachelor's degree in biology from the University of California, San Diego; a master's degree in infectious disease from the University of California, Berkeley; and a doctoral degree in biochemistry and molecular biophysics from the California Institute of Technology.



**Gregory A. Ciccarelli** is a technical staff member in the Human Health and Performance Systems Group. He works on neurocomputational modeling, using model-based approaches to study depression, Parkinson's disease, traumatic brain injury, and auditory health. He holds a doctoral degree from MIT; his

dissertation characterized why speech is a good biomarker of neuropsychological disorders.



**Shaun R. Berry** is a technical staff member in the Advanced Materials and Microsystems Group. He has worked on a variety of microelectromechanical systems and microfluidic projects, which have included developing microelectromechanical microswitches, variable-focus liquid lenses, micropumps, and non-

mechanical beam-steering devices. He is currently interested in developing microsystems for active optical devices, communications, and microhydraulics. He holds a bachelor's degree in mechanical engineering from Northeastern University and master's and doctoral degrees in mechanical engineering from Tufts University. His doctoral research was focused on microfluidics and the electrowetting phenomenon.



**Jeffrey S. Palmer** is the leader of the Human Health and Performance Systems Group at Lincoln Laboratory. He has oversight of multiple research programs that focus on health, human performance, objective neurocognitive analytics, and biosensing via wearable, ingestible, and implantable devices. In

2010, he helped to create the first Army War College Fellowship at Lincoln Laboratory and the MIT Security Studies Program. He has given presentations at international conferences and authored book chapters and technical articles on DNA biometrics and forensics, biomechanics, cell biology, materials science, soldier nanotechnology, biological-chemical defense, polymer science, high-energy lasers, microelectronics packaging, wearable biomedical sensing in extreme environments, and neurocognitive technologies. He has served on editorial boards for journals in biomechanics, molecular science, biomedical informatics, and biosensors. He has chaired technical conferences for the National Science Foundation, Department of Homeland Security, and the IEEE. Currently, he is the vice chair (and chair-elect) of the IEEE Engineering in Medicine and Biology Society's (EMBS) Technical Committee on Wearable Biomedical Sensors and Systems and the EMBS conference editorial board for tissue engineering and biomaterials. In addition, he has served as an advisor on senior military studies of enhancing health and performance, and led a multi-agency U.S. government effort to develop automated rapid

human DNA analysis capabilities for field biometrics and forensics applications. Prior to working at Lincoln Laboratory, he worked at research laboratories at IBM and GE, and at the Physical Sciences Laboratory at New Mexico State University. He holds a bachelor's degree with a minor in mathematics from New Mexico State University, a master's degree from Rensselaer Polytechnic Institute, and a doctorate with a minor in bioengineering from MIT, all with majors in mechanical engineering.



**Satrajit Ghosh** is a principal research scientist at the McGovern Institute for Brain Research at MIT and an assistant professor in the Department of Otolaryngology at Harvard Medical School. He is also the director of the Data Models and Integration project of ReproNim, a National Institutes of

Health P41 Center for Reproducible Neuroimaging Computation. His research interests span computer science and neuroimaging, specifically in the areas of applied machine learning, software engineering, and applications of neuroimaging. The primary focus of his research group is to develop platforms for knowledge discovery by integrating a set of multidisciplinary projects that span precision medicine in mental health, imaging genetics, machine learning, and dataflow systems for reproducible research. He is a lead architect of the Nipype dataflow platform; an ardent proponent of decentralized and distributed web solutions for data sharing, querying, and computing; and a strong believer in solving problems through collaboration and crowdsourcing. To help accelerate building an open Commons for neuroscience, he is currently serving as a co-editor-in-chief for a new journal, *BMC NeuroCommons*.



**Kwanghun Chung** is an assistant professor of chemical engineering at the MIT Institute for Medical Engineering and Science and a principal investigator at the Picower Institute for Learning and Memory. He is a co-inventor of a novel technology termed CLARITY, which enables system-wide structural

and molecular analysis of large-scale intact biological samples, including rodent brains and human clinical samples. His research laboratory at MIT is an interdisciplinary research team devoted to developing and applying novel technologies for integrative and comprehensive understanding of large-scale, complex biological systems. He holds a doctoral degree from the Georgia Institute of Technology and completed his postdoctoral training at the Karl Deisseroth Lab at Stanford University.